AGU PUBLICATIONS

Geophysical Research Letters

RESEARCH LETTER
10.1002/2016GL070194

Key Points:
- Energetic electron angular distribution evolution during a geomagnetic storm
- Gyroresonant interaction between whistler-mode chorus and energetic electrons
- Chorus acceleration can rapidly flatten the butterfly angular distribution

Correspondence to:
Z. Su,
szpe@mail.ustc.edu.cn

Citation:
Yang, C., et al. (2016), Rapid flattening of butterfly pitch angle distributions of radiation belt electrons by whistler-mode chorus, *Geophys. Res. Lett.*, *43*, 8339–8347, doi:10.1002/2016GL070194.

Received 27 JUN 2016
Accepted 11 AUG 2016
Accepted article online 16 AUG 2016
Published online 25 AUG 2016

Rapid flattening of butterfly pitch angle distributions of radiation belt electrons by whistler-mode chorus

Chang Yang[1,2,3], Zhenpeng Su[1,2], Fuliang Xiao[3], Huinan Zheng[1,2], Yuming Wang[1,2], Shui Wang[1,2], H. E. Spence[4], G. D. Reeves[5,6], D. N. Baker[7], J. B. Blake[8], and H. O. Funsten[9]

[1]Department of Geophysics and Planetary Sciences, University of Science and Technology of China, Hefei, China, [2]Collaborative Innovation Center of Astronautical Science and Technology, University of Science and Technology of China, Hefei, China, [3]School of Physics and Electronic Sciences, Changsha University of Science and Technology, Changsha, China, [4]Institute for the Study of Earth, Oceans, and Space, University of New Hampshire, Durham, New Hampshire, USA, [5]Space Science and Applications Group, Los Alamos National Laboratory, Los Alamos, New Mexico, USA, [6]Space Sciences Division, The New Mexico Consortium, Los Alamos, New Mexico, USA, [7]Laboratory for Atmospheric and Space Physics, University of Colorado Boulder, Boulder, Colorado, USA, [8]Aerospace Corporation, Los Angeles, California, USA, [9]ISR Division, Los Alamos National Laboratory, Los Alamos, New Mexico, USA

Abstract Van Allen radiation belt electrons exhibit complex dynamics during geomagnetically active periods. Investigation of electron pitch angle distributions (PADs) can provide important information on the dominant physical mechanisms controlling radiation belt behaviors. Here we report a storm time radiation belt event where energetic electron PADs changed from butterfly distributions to normal or flattop distributions within several hours. Van Allen Probes observations showed that the flattening of butterfly PADs was closely related to the occurrence of whistler-mode chorus waves. Two-dimensional quasi-linear STEERB simulations demonstrate that the observed chorus can resonantly accelerate the near-equatorially trapped electrons and rapidly flatten the corresponding electron butterfly PADs. These results provide a new insight on how chorus waves affect the dynamic evolution of radiation belt electrons.

1. Introduction

Energetic electron fluxes in the outer Van Allen radiation belt are highly dynamic [e.g., *Baker et al.*, 1986, 2013; *Li et al.*, 2001; *Reeves et al.*, 2003; *Anderson et al.*, 2015] due to various transport [*Fälthammar*, 1965; *Elkington et al.*, 1999; *Huang et al.*, 2010; *Mann et al.*, 2013; *Su et al.*, 2015], acceleration [e.g., *Summers et al.*, 2002; *Horne et al.*, 2005; *Omura et al.*, 2007; *Bortnik et al.*, 2008] and loss [e.g., *Shprits et al.*, 2006; *Bortnik et al.*, 2006; *Millan et al.*, 2007; *Su et al.*, 2011a, 2012, 2016; *Hudson et al.*, 2014; *Zhu et al.*, 2015] processes. Pitch angle α is an essential parameter to describe charged particle motions in the terrestrial magnetic field. Investigation of electron pitch angle distributions (PADs) can help us to better understand the dominant physical mechanisms controlling radiation belt behaviors.

In general, three types of electron PADs occur frequently in the magnetosphere [*West et al.*, 1973; *Sibeck et al.*, 1987; *Horne et al.*, 2003; *Gannon et al.*, 2007; *Su et al.*, 2009; *Thorne et al.*, 2010; *Gu et al.*, 2011; *Zhao et al.*, 2014; *Ni et al.*, 2015]: (1) normal distribution with a flux peak around $\alpha = 90°$; (2) flattop distribution with nearly isotropic fluxes at large pitch angles; (3) butterfly distribution with a flux minimum around $\alpha = 90°$. Formation of butterfly PADs has received much attention in the past, and various adiabatic and nonadiabatic candidate mechanisms have been proposed: fully adiabatic transport [*Su et al.*, 2010a, 2011b], drift shell splitting [*Sibeck et al.*, 1987; *Selesnick and Blake*, 2002; *Yu et al.*, 2016], magnetic field line curvature scattering [*Artemyev et al.*, 2015], Landau [*Horne et al.*, 2007; *Xiao et al.*, 2015; *Li et al.*, 2016], and nonlinear bounce [*Maldonado et al.*, 2016] resonance with magnetosonic waves, nonlinear Landau resonance with oblique electromagnetic ion cyclotron waves [*Wang et al.*, 2016], and Landau/cyclotron resonance with plasmaspheric hiss, lightning-generated whistlers, and very low frequency transmitters [*Albert et al.*, 2016]. However, relatively few studies have been performed to investigate the recovery process from butterfly PADs to normal/flattop PADs.

In this study, we report a radiation belt event with the rapid flattening of electron butterfly PADs during the geomagnetic storm on 24 February 2015. Based on comprehensive observations of Van Allen Probes

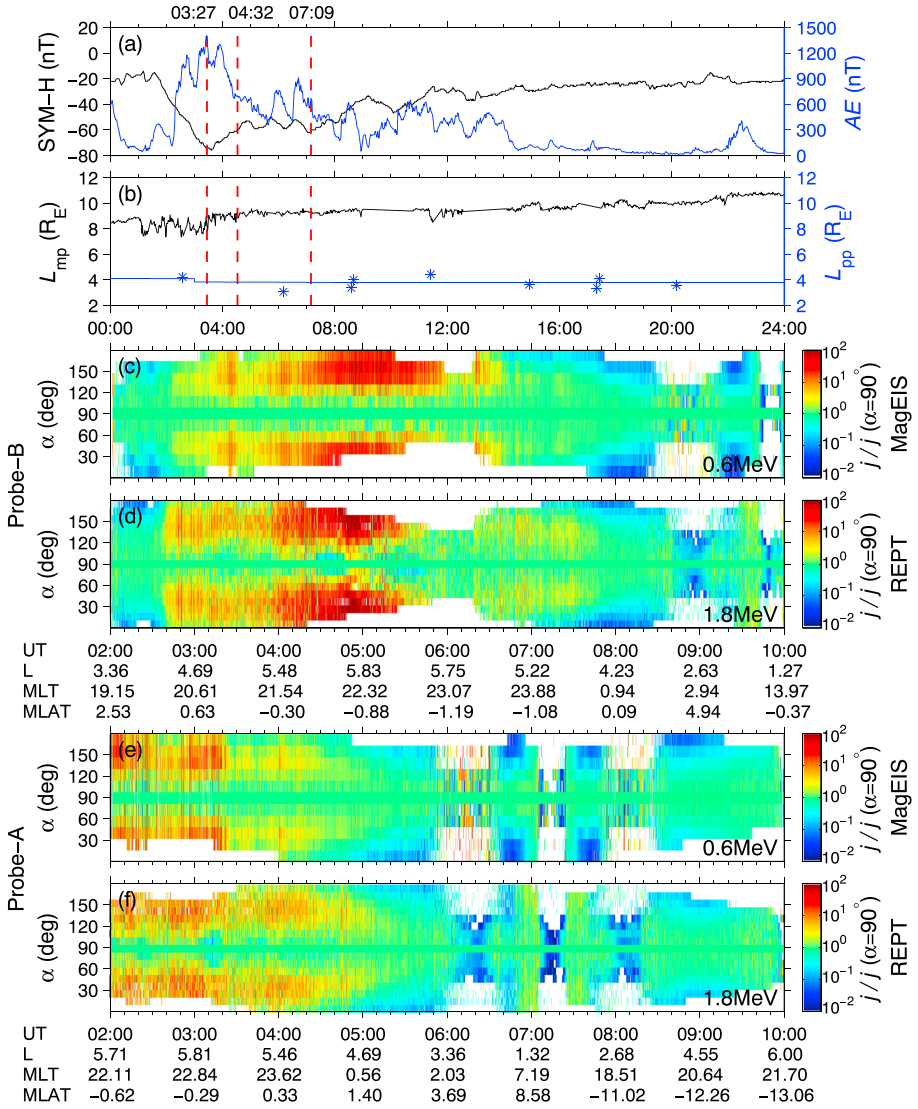

Figure 1. Overview of the radiation belt event on 24 February 2015: (a) Geomagnetic activity indices *SYM-H* (black) and *AE* (blue); (b) Subsolar magnetopause location L_{mp} (black) and nightside plasmapause location L_{pp} (blue); (c–f) Normalized electron differential fluxes $j/j(\alpha=90°)$ at 0.6 MeV and 1.8 MeV measured by twin Van Allen Probes. The vertical red lines in Figures 1a and 1b denote the times when Van Allen Probes passed through the location $L=5.1$.

[*Mauk et al.*, 2013] and quasi-linear simulations of STEERB model [*Su et al.*, 2010b], we attempt to determine the dominant mechanism for electron PAD evolution in this event.

2. Observations

On 24 February 2015, the magnetosphere experienced a moderate geomagnetic storm with the minimum *SYM-H*≈−76 nT and some strong substorms with the maximum *AE*≈1400 nT (Figure 1a). The subsolar magnetopause L_{mp} (estimated based on interplanetary parameters [*Shue et al.*, 1998]) was compressed to about 7.5 R_E during the main phase and returned back to 9 R_E during the recovery phase (black line in Figure 1b). As inferred from the spacecraft potential measurements of Electric Field and Waves (EFW) instrument (blue symbols in Figure 1b) of twin Van Allen Probes and modeled based on the *Dst* index [*O'Brien and Moldwin*, 2003] (blue line in Figure 1b), the nightside plasmapause was located around $L = 4$ throughout the day.

Radiation belt electron fluxes were observed by Magnetic Electron Ion Spectrometer (MagEIS) [*Blake et al.*, 2013] and Relativistic Electron-Proton Telescope (REPT) [*Baker et al.*, 2012] of Energetic Particle, Composition, and Thermal Plasma (ECT) suite [*Spence et al.*, 2013] of twin Van Allen Probes. To clearly identify electron

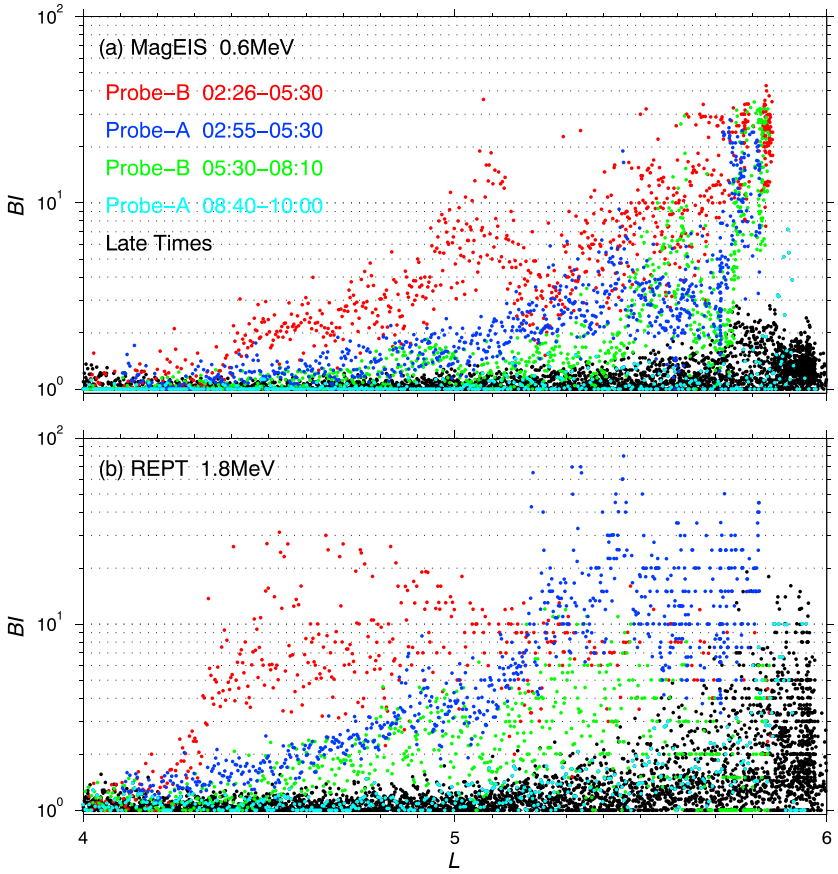

Figure 2. *L*-dependent butterfly index *BI* derived from twin Van Allen Probes observations during different time ranges.

PAD characteristics, we show the normalized fluxes $j(\alpha)/j(\alpha=90°)$ at two energy channels 0.6 and 1.8 MeV (Figures 1c–1f). To quantitatively describe the patterns of electron PADs, we introduce a butterfly index $BI=\max\{j(\alpha)/j(\alpha=90°)\}$ (Figure 2). Butterfly index *BI* would become larger for more distinct butterfly PADs, and degenerate into 1 for normal/flattop PADs. During the period of 02:40–06:00 UT (Figures 1c–1f), radiation belt electrons at nightside relatively large *L* shells ($L \geq 4.4$) displayed distinct butterfly distributions with minima near the pitch angle $\alpha = 90°$ and peaks in the pitch angle range of $|\alpha - 90°| = 40° - 70°$. From the higher to lower *L* shells, the butterfly distributions gradually turned flat and exhibited normal/flattop patterns in the region $L < 4.2$. Note that *L* is defined as the geocentric equatorial radial distance of TS04-modeled [*Tsyganenko and Sitnov*, 2005] geomagnetic magnetic field lines. Given the highly compressed magnetosphere (Figure 1b), the observed butterfly distributions are considered to be caused by the drift shell splitting [*Sibeck et al.*, 1987; *Selesnick and Blake*, 2002] and magnetopause shadowing [*Li et al.*, 1997; *Desorgher et al.*, 2000; *Hudson et al.*, 2014]. During the period of 06:30–08:30 UT (Figures 1c–1f), the butterfly PADs were found to be flattened significantly. At a given *L*-shell $L = 5.1$, *BI* index decreased by up to one order of magnitude within several hours (Figures 2). In the next tens of hours, *BI* remained close to 1 at $L \leq 5.5$ (Figure 2).

Plasma waves were detected by Electric and Magnetic Field Instrument Suite and Integrated Science (EMFISIS) suite [*Kletzing et al.*, 2013] of twin Van Allen Probes. During 03:30–08:00 UT, in response to strong substorm activities (Figure 1a), enhanced whistler-mode chorus waves in the frequency range 0.05–0.65 f_{ce} occurred over a broad range of MLT and *L* shells (Figure 3). Note that f_{ce} is the equatorial electron gyrofrequency calculated as

$$f_{ce} = \frac{eB_e}{2\pi m} = \frac{eB_o}{2\pi m}\frac{B_{Me}}{B_{Mo}}, \tag{1}$$

with the local magnetic field B_o observed by Van Allen Probes and the ratio B_{Me}/B_{Mo} of equatorial to local field strengths in the TS04 model. As suggested in previous works [e.g., *Summers et al.*, 2002; *Horne et al.*, 2005;

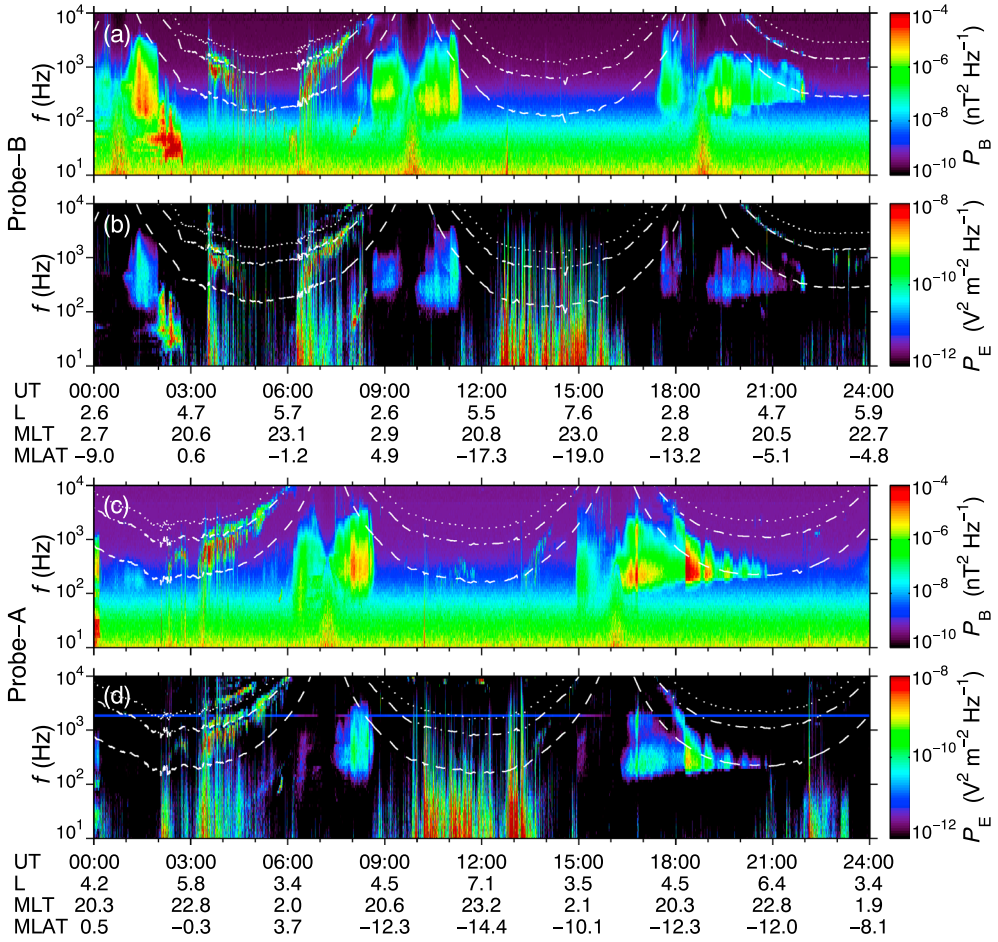

Figure 3. Wave magnetic P_B and electric P_E power spectral density measured by twin Van Allen Probes on 24 February 2015. The white lines represent f_{ce} (dotted), $0.5f_{ce}$ (dashed-dotted), and $0.1f_{ce}$ (dashed), respectively.

Li et al., 2007; *Reeves et al.*, 2013; *Thorne et al.*, 2013; *Su et al.*, 2014a], the chorus waves can resonantly accelerate radiation belt electrons particularly at pitch angles near $\alpha = 90°$. After 03:30 UT, the drift loss to magnetopause became quite weak for a relaxed magnetosphere ($L_{mp} > 9$ in Figure 1b) and the chorus-driven acceleration can be expected to fill the concave part of butterfly PADs near $\alpha = 90°$ [*Horne et al.*, 2003].

3. Simulations

We use the two-dimensional STEERB model [*Su et al.*, 2010b, 2011c] to simulate the flattening of butterfly PADs by whistler-mode chorus at $L = 5.1$ (where the maximum butterfly index *BI* was observed). The basic equation is the drift-averaged Fokker-Planck equation [e.g., *Xiao et al.*, 2009]

$$\frac{\partial F}{\partial t} = \frac{1}{Gp}\frac{\partial}{\partial \alpha_e}\left[G\left(\langle D_{\alpha\alpha}\rangle \frac{1}{p}\frac{\partial F}{\partial \alpha_e} + \langle D_{\alpha p}\rangle \frac{\partial F}{\partial p}\right)\right] + \frac{1}{G}\frac{\partial}{\partial p}\left[G\left(\langle D_{p\alpha}\rangle \frac{1}{p}\frac{\partial F}{\partial \alpha_e} + \langle D_{pp}\rangle \frac{\partial F}{\partial p}\right)\right] \quad (2)$$

Electron phase space density F is a function of equatorial pitch angle α_e and momentum p. To allow the model-to-data comparison of electron fluxes $j = p^2F$, the local pitch angle α is mapped to the equatorial pitch angle α_e based on the assumption of conserving the first adiabatic invariant in the TS04-modeled magnetic field. Efficiency of gyroresonance between whistler-mode chorus and energetic electrons is described by the drift-averaged diffusion coefficients in pitch angle $\langle D_{\alpha\alpha}\rangle$, momentum $\langle D_{pp}\rangle$, and cross term $\langle D_{\alpha p}\rangle = \langle D_{p\alpha}\rangle$ [e.g., *Kennel and Engelmann*, 1966; *Horne and Thorne*, 1998; *Summers et al.*, 1998; *Albert*, 2005].

To calculate the drift-averaged diffusion coefficients, we need to know the characteristics of background plasma and chorus waves. We take the equatorial magnetic field amplitude B_e=120 nT based on the

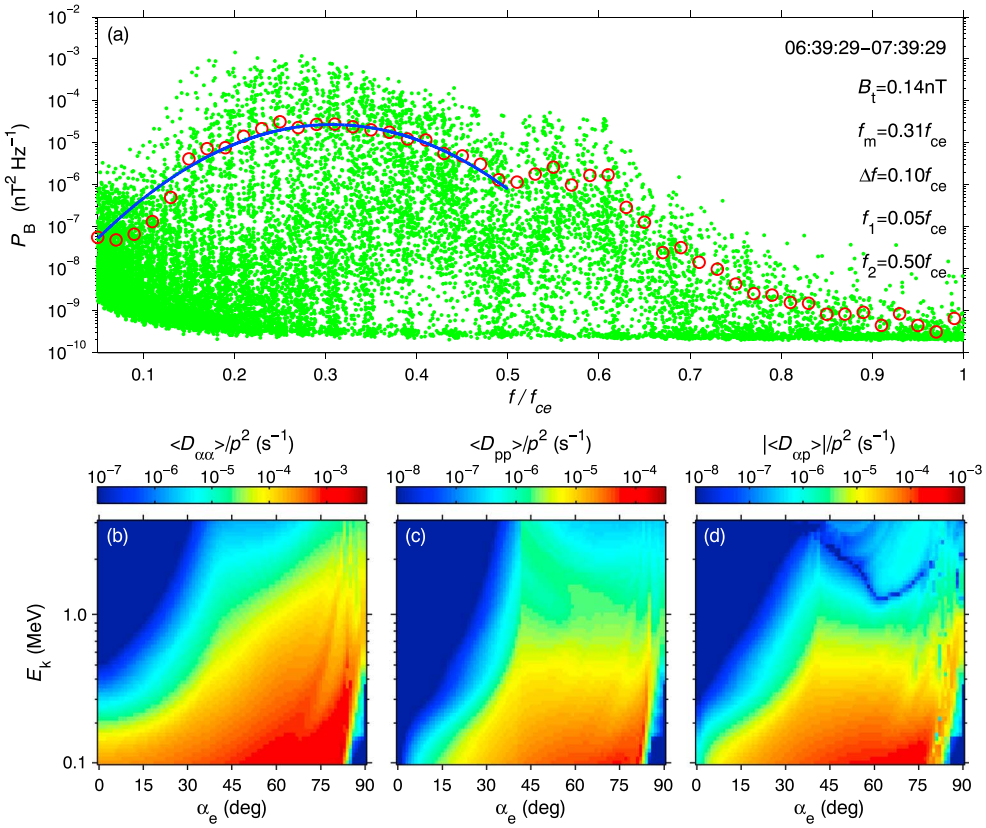

Figure 4. (a) Gaussian fitting (blue line) to the time-averaged (red circles) magnetic wave power spectra P_B (green dots); (b-d) drift-averaged diffusion rates $\langle D_{\alpha\alpha}\rangle/p^2$, $\langle D_{pp}\rangle/p^2$, and $|\langle D_{\alpha p}\rangle|/p^2$ of modeled chorus as functions of kinetic energy E_k and equatorial pitch angle α_e.

observations and assume that the field-aligned magnetic amplitude follows the dipole field. The ambient plasma density n_e=4.8 cm^{-3} is inferred from the upper hybrid resonance frequency measured by EMFISIS suite [*Kurth et al.*, 2015]. Based on early works [e.g., *Horne et al.*, 2005; *Li et al.*, 2007; *Shprits et al.*, 2009], the latitudinal range and longitudinal occurrence rate of chorus waves are empirically set as $|\lambda|<25°$ and 20%. The tangent of wave normal angle $X=\tan\theta$ is assumed to obey a typical Gaussian distribution [*Horne et al.*, 2005] with a lower cutoff $X_1=0$, an upper cutoff $X_2=1$, a center $X_m=0$ and a half-width $\Delta X=0.577$. Following our previous works [*Su et al.*, 2014b, 2014c; *Gao et al.*, 2016], wave spectra are averaged over a 1 h period of 06:39:29–07:39:29 UT around $L=5.1$ near the midnight to obtain a Gaussian distribution [*Lyons and Thorne*, 1972; *Lyons*, 1974] with an amplitude $B_t=0.14$ nT, a lower cutoff frequency $f_1=0.05f_{ce}$, an upper cutoff $f_2=0.50f_{ce}$, a center $f_m=0.31f_{ce}$, and a half-width $\Delta f=0.10f_{ce}$ (Figure 4a). Using the plasma and wave parameters above, we can calculate the local diffusion coefficients for Landau ($n=0$) and cyclotron harmonic ($n=\pm1,\ \pm2,\ldots,\ \pm5$) resonances at arbitrary positions [see *Glauert and Horne*, 2005, equations (8)–(13)] and then obtain the drift-averaged diffusion coefficients [see *Glauert and Horne*, 2005, equations (21)–(23)] by averaging over electron bounce and drift orbit. The drift-averaged diffusion rates (Figures 4b–4d) tend to be more pronounced at relatively larger pitch angles than those at smaller pitch angles, indicating that chorus-induced diffusive acceleration processes are more efficient for near-equatorially trapped electrons.

The computational domain is chosen as $E_k\in$(0.1 MeV, 3.0 MeV)×$\alpha_e\in(0°, 90°)$. The boundary conditions are set as follows: $F=0$ at the loss cone $\alpha=\alpha_L$, $\partial F/\partial\alpha_e=0$ at $\alpha_e=90°$, $F=$const at $E_k=0.1$ MeV, and $\partial F/\partial p=0$ at $E_k=3$ MeV. The simulation is initialized at 03:27:03 UT and ended at 07:09:29 UT. In this time range, Van Allen Probes cannot collect data reflecting the electron PAD flattening at a fixed location. For the following comparison between simulation results and experimental data, we have ignored the potential longitudinal variation of electron PADs in the region MLT = 21–24. The initial electron distribution (Figure 5a) is interpolated from the observations around 03:27:03 UT on 24 February 2015 (Probe B, $L=5.1$, MLT = 21.1, and MLAT = 0.1°). At the intermediate (Probe A, 04:32:21 UT, $L=5.1$, MLT = 0.1, and MLAT = 0.8°) and final states

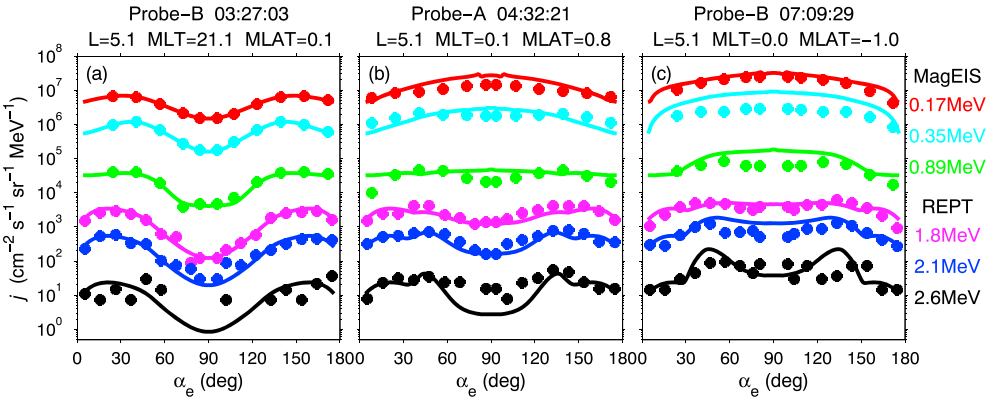

Figure 5. Comparison between observed (dotted) and simulated (lines) differential fluxes *j* at the (a) initial, (b) intermediate, and (c) final states. Note that the experimental data have been smoothed over 2 min.

(Probe B, 07:09:29 UT, $L = 5.1$, MLT = 0.0, and MLAT = −1.0°), the simulations show a reasonable agreement with observations from both Van Allen Probes (Figures 5b and 5c). As a result of the monotonically decreasing diffusion intensity with increasing energy, the flattening of electron PADs tends to occur earlier at lower energy channels. At the pitch angles near $\alpha_e = 90°$ with strong diffusion, the electron fluxes are enhanced by up to 10 times; at the pitch angles $|\alpha_e - 90°| > 45°$ with quite weak diffusion, the electron fluxes remain nearly unchanged. These results clearly illustrate that the chorus-driven resonant acceleration process can effectively flatten the radiation belt electron butterfly PADs within several hours.

4. Conclusion and Discussion

Electron PAD pattern is an important indicator of radiation belt dynamics. In the past, many observational and theoretical works [e.g., *Sibeck et al.*, 1987; *Selesnick and Blake*, 2002; *Su et al.*, 2010a; *Artemyev et al.*, 2015; *Xiao et al.*, 2015; *Maldonado et al.*, 2016; *Wang et al.*, 2016; *Albert et al.*, 2016] have been presented to explain the formation of butterfly electron PADs. Here we focus on the evolution of PADs from butterfly patterns to normal/flattop patterns observed by Van Allen Probes during a geomagnetic storm on 24 February 2015. During the main phase, the subsolar magnetopause was compressed to $L_{mp} = 7.5$ and the electron butterfly PADs formed at relatively large *L* shells probably due to the drift shell splitting and magnetopause shadowing. During the recovery phase, the subsolar magnetopause returned to $L_{mp} > 9$ and the electron butterfly PADs at $L = 5.1$ were rapidly flattened within 4 h. Simultaneously, intense whistler-mode chorus waves occurred over a broad spatial region ($L = 4.3–5.8$). These chorus waves are found to be able to accelerate the energetic electrons at the pitch angles $|\alpha_e - 90°| < 45°$ through the gyroresonance. Taking into account the chorus-driven resonant acceleration process, STEERB model can well reproduce the observed flattening of electron butterfly PADs on a short timescale. Our results clearly illustrate the important role of whistler-mode chorus waves in the radiation belt dynamics from a new point of view.

In this study, the chorus-driven local acceleration is quantified in the quasi-linear framework [e.g., *Kennel and Engelmann*, 1966; *Horne and Thorne*, 1998; *Summers et al.*, 1998; *Albert*, 2005]. In fact, the chorus waves often consist of discrete rising tone elements with large amplitudes of several nanotesla [*Cattell et al.*, 2008; *Cully et al.*, 2008; *Santolík et al.*, 2014], allowing the action of nonlinear acceleration [e.g., *Omura et al.*, 2007; *Summers and Omura*, 2007; *Bortnik et al.*, 2008]. Recent test particle simulation of *Omura et al.* [2015] has suggested that the nonlinear chorus acceleration can produce a butterfly (rather than a flattop) electron PAD. This discrepancy may be caused by the difference of simulation parameters (wave amplitude, frequency and normal angle characteristics, background plasma condition, and initial state). Future test particle simulations with realistic wave fine structures [*Santolík et al.*, 2014] and event-specific conditions are required to examine the quasi-linear simulation results.

Radial diffusion driven by ultralow-frequency waves [e.g., *Fälthammar*, 1965; *Elkington et al.*, 1999; *Hudson et al.*, 2000] is a competing mechanism to the chorus-driven local acceleration. Recent observations of Van Allen Probes have shown strong evidence for the action of radial diffusion during both storm [*Mann et al.*, 2016] and non-storm [*Su et al.*, 2015] times. The radial diffusion rate is usually considered to weakly depend on the equatorial pitch angle [e.g., *Brautigam and Albert*, 2000; *Ozeke et al.*, 2014]. To preferentially enhance

the equatorially trapped electron fluxes by radial diffusion, electron phase space density is required to have a stronger positive radial gradient at a smaller K invariant (i.e., at a pitch angle closer to $\alpha_e = 90°$). It would seem hard to satisfy this condition after the magnetopause shadowing (yielding stronger loss at pitch angles closer to $\alpha_e = 90°$ in the nightside region [*Hudson et al.*, 2014]). Nevertheless, accurate evaluation of the contribution of radial diffusion to electron PAD flattening is left for future works.

Adiabatic process in response to background magnetic field variation is another possible cause of electron PAD evolution [e.g., *Su et al.*, 2010a; *Yu et al.*, 2016]. A weaker drift shell splitting effect can be expected in a less stretched magnetic field. The competition and cooperation of these adiabatic and nonadiabatic (radial diffusion and chorus acceleration) mechanisms should be investigated using the global radiation belt models in a realistic time-varying geomagnetic field.

Acknowledgments
This work was supported by the National Natural Science Foundation of China grants 41422405, 41274169, 41274174, 41174125, 41131065, 41421063, 41231066, and 41304134, the Chinese Academy of Sciences grant KZCX2-EW-QN510 and KZZD-EW-01-4, the National Key Basic Research Special Foundation of China grant 2011CB811403, and the Fundamental Research Funds for the Central Universities WK2080000077. Data are available at the following websites: http://cdaweb.gsfc.nasa.gov/cdaweb/istp_public/ (geomagnetic activity indices), http://emfisis.physics.uiowa.edu/Flight/ (EMFISIS), http://www.rbsp-ect.lanl.gov/data_pub/ (ECT), and http://www.space.umn.edu/rbspefw-data/ (EFW).

References

Albert, J. M. (2005), Evaluation of quasi-linear diffusion coefficients for whistler mode waves in a plasma with arbitrary density ratio, *J. Geophys. Res.*, *110*, A03218, doi:10.1029/2004JA010844.

Albert, J. M., R. B. M. P. Starks, M. J. Horne, and S. A. Glauert (2016), Quasi-linear simulations of inner radiation belt electron pitch angle and energy distributions, *Geophys. Res. Lett.*, *43*, 2381–2388, doi:10.1002/2016GL067938.

Anderson, B. R., R. Millan, G. D. Reeves, and R. H. W. Friedel (2015), Acceleration and loss of relativistic electrons during small geomagnetic storms, *Geophys. Res. Lett.*, *42*, 10,113–10,119, doi:10.1002/2015GL066376.

Artemyev, A. V., O. V. Agapitov, F. S. Mozer, and H. Spence (2015), Butterfly pitch angle distribution of relativistic electrons in the outer radiation belt: Evidence of nonadiabatic scattering, *J. Geophys. Res.Space Physics*, *120*, 4279–4297, doi:10.1002/2014JA020865.

Baker, D. N., R. W. Klebesadel, P. R. Higbie, and J. B. Blake (1986), Highly relativistic electrons in the Earth's outer magnetosphere. I—Lifetimes and temporal history 1979–1984, *J. Geophys. Res.*, *91*, 4265–4276, doi:10.1029/JA091iA04p04265.

Baker, D. N., et al. (2012), The relativistic electron-proton telescope (REPT) instrument on board the Radiation Belt Storm Probes (RBSP) spacecraft: Characterization of Earth's radiation belt high-energy particle populations, *Space Sci. Rev.*, *179*, 337–381, doi:10.1007/s11214-012-9950-9.

Baker, D. N., et al. (2013), A long-lived relativistic electron storage ring embedded in Earth's outer Van Allen belt, *Science*, *340*, 186–190, doi:10.1126/science.1233518.

Blake, J. B., et al. (2013), The magnetic electron ion spectrometer (MagEIS) instruments aboard the radiation belt storm probes (RBSP) spacecraft, *Space. Sci. Rev.*, *179*, 383–421, doi:10.1007/s11214-013-9991-8.

Bortnik, J., R. M. Thorne, T. P. O'Brien, J. C. Green, R. J. Strangeway, Y. Y. Shprits, and D. N. Baker (2006), Observation of two distinct, rapid loss mechanisms during the 20 November 2003 radiation belt dropout event, *J. Geophys. Res.*, *111*, A12216, doi:10.1029/2006JA011802.

Bortnik, J., R. M. Thorne, and U. S. Inan (2008), Nonlinear interaction of energetic electrons with large amplitude chorus, *Geophys. Res. Lett.*, *35*, L21102, doi:10.1029/2008GL035500.

Brautigam, D. H., and J. M. Albert (2000), Radial diffusion analysis of outer radiation belt electrons during the October 9, 1990, magnetic storm, *J. Geophys. Res.*, *105*, 291–310, doi:10.1029/1999JA900344.

Cattell, C., et al. (2008), Discovery of very large amplitude whistler-mode waves in Earth's radiation belts, *Geophys. Res. Lett.*, *35*, L01105, doi:10.1029/2007GL032009.

Cully, C. M., J. W. Bonnell, and R. E. Ergun (2008), THEMIS observations of long-lived regions of large-amplitude whistler waves in the inner magnetosphere, *Geophys. Res. Lett.*, *35*, L17S16, doi:10.1029/2008GL033643.

Desorgher, L., P. Bühler, A. Zehnder, and E. O. Flückiger (2000), Simulation of the outer radiation belt electron flux decrease during the March 26, 1995, magnetic storm, *J. Geophys. Res.*, *105*, 21,211–21,224, doi:10.1029/2000JA900060.

Elkington, S. R., M. K. Hudson, and A. A. Chan (1999), Acceleration of relativistic electrons via drift-resonant interaction with toroidal-mode Pc-5 ULF oscillations, *Geophys. Res. Lett.*, *26*, 3273–3276, doi:10.1029/1999GL003659.

Fälthammar, C.-G. (1965), Effects of time-dependent electric fields on geomagnetically trapped radiation, *J. Geophys. Res.*, *70*, 2503–2516, doi:10.1029/JZ070i011p02503.

Gannon, J. L., X. Li, and D. Heynderickx (2007), Pitch angle distribution analysis of radiation belt electrons based on combined release and radiation effects satellite medium electrons a data, *J. Geophys. Res.*, *112*, A05212, doi:10.1029/2005JA011565.

Gao, Z., Z. Su, H. Zhu, F. Xiao, H. Zheng, Y. Wang, C. Shen, and S. Wang (2016), Intense low-frequency chorus waves observed by Van Allen Probes: Fine structures and potential effect on radiation belt electrons, *Geophys. Res. Lett.*, *43*, 967–977, doi:10.1002/2016GL067687.

Glauert, S. A., and R. B. Horne (2005), Calculation of pitch angle and energy diffusion coefficients with the PADIE code, *J. Geophys. Res.*, *110*, A04206, doi:10.1029/2004JA010851.

Gu, X., Z. Zhao, B. Ni, Y. Y. Shprits, and C. Zhou (2011), Statistical analysis of pitch angle distribution of radiation belt energetic electrons near the geostationary orbit: Crres observations, *J. Geophys. Res.*, *116*, A01208, doi:10.1029/2010JA016052.

Horne, R. B., and R. M. Thorne (1998), Potential waves for relativistic electron scattering and stochastic acceleration during magnetic storms, *Geophys. Res. Lett.*, *25*, 3011–3014, doi:10.1029/98GL01002.

Horne, R. B., N. P. Meredith, R. M. Thorne, D. Heynderickx, R. H. A. Iles, and R. R. Anderson (2003), Evolution of energetic electron pitch angle distributions during storm time electron acceleration to megaelectronvolt energies, *J. Geophys. Res.*, *108*(A1), 1016, doi:10.1029/2001JA009165.

Horne, R. B., et al. (2005), Wave acceleration of electrons in the Van Allen radiation belts, *Nature*, *437*, 227–230, doi:10.1038/nature03939.

Horne, R. B., R. M. Thorne, S. A. Glauert, J. M. Albert, N. P. Meredith, and R. R. Anderson (2005), Timescale for radiation belt electron acceleration by whistler mode chorus waves, *J. Geophys. Res.*, *110*, A03225, doi:10.1029/2004JA010811.

Horne, R. B., R. M. Thorne, S. A. Glauert, N. P. Meredith, D. Pokhotelov, and O. Santolík (2007), Electron acceleration in the Van Allen radiation belts by fast magnetosonic waves, *Geophys. Res. Lett.*, *34*, L17107, doi:10.1029/2007GL030267.

Huang, C.-L., H. E. Spence, M. K. Hudson, and S. R. Elkington (2010), Modeling radiation belt radial diffusion in ULF wave fields: 2. Estimating rates of radial diffusion using combined MHD and particle codes, *J. Geophys. Res.*, *115*, A06216, doi:10.1029/2009JA014918.

Hudson, M. K., S. R. Elkington, J. G. Lyon, and C. C. Goodrich (2000), Increase in relativistic electron flux in the inner magnetosphere: ULF wave mode structure, *Adv. Space Res.*, *25*, 2327–2337, doi:10.1016/S0273-1177(99)00518-9.

Hudson, M. K., D. N. Baker, J. Goldstein, B. T. Kress, J. Paral, F. R. Toffoletto, and M. Wiltberger (2014), Simulated magnetopause losses and Van Allen Probe flux dropouts, *Geophys. Res. Lett.*, *41*, 1113–1118, doi:10.1002/2014GL059222.

Kennel, C. F., and F. Engelmann (1966), Velocity space diffusion from weak plasma turbulence in a magnetic field, *Phys. Fluids*, *9*, 2377–2388, doi:10.1063/1.1761629.

Kletzing, C. A., et al. (2013), The Electric and Magnetic Field Instrument Suite and Integrated Science (EMFISIS) on RBSP, *Space Sci. Rev.*, *179*, 127–181, doi:10.1007/s11214-013-9993-6.

Kurth, W. S., S. D. Pascuale, J. B. Faden, C. A. Kletzing, G. B. Hospodarsky, S. Thaller, and J. R. Wygant (2015), Electron densities inferred from plasma wave spectra obtained by the waves instrument on Van Allen Probes, *J. Geophys. Res. Space Physics*, *120*, 904–914, doi:10.1002/2014JA020857.

Li, J., et al. (2016), Formation of energetic electron butterfly distributions by magnetosonic waves via Landau resonance, *Geophys. Res. Lett.*, *43*, 3009–3016, doi:10.1002/2016GL067853.

Li, W., Y. Y. Shprits, and R. M. Thorne (2007), Dynamic evolution of energetic outer zone electrons due to wave-particle interactions during storms, *J. Geophys. Res.*, *112*, A10220, doi:10.1029/2007JA012368.

Li, X., D. N. Baker, M. Temerin, T. E. Cayton, E. G. D. Reeves, R. A. Christensen, J. B. Blake, M. D. Looper, R. Nakamura, and S. G. Kanekal (1997), Multisatellite observations of the outer zone electron variation during the November 3–4, 1993, magnetic storm, *J. Geophys. Res.*, *102*, 14,123–14,140, doi:10.1029/97JA01101.

Li, X., D. N. Baker, S. G. Kanekal, M. Looper, and M. Temerin (2001), Long term measurements of radiation belts by SAMPEX and their variations, *Geophys. Res. Lett.*, *28*, 3827–3830, doi:10.1029/2001GL013586.

Lyons, L. R. (1974), Pitch angle and energy diffusion coefficients from resonant interactions with ion-cyclotron and whistler waves, *J. Plasma Phys.*, *12*, 417–432.

Lyons, L. R., and R. M. Thorne (1972), Parasitic pitch angle diffusion of radiation belt particles by ion cyclotron waves, *J. Geophys. Res.*, *77*, 5608–5616.

Maldonado, A. A., L. Chen, and S. G. Claudepierre (2016), Electron butterfly distribution modulation by magnetosonic waves, *Geophys. Res. Lett.*, *43*, 3051–3059, doi:10.1002/2016GL068161.

Mann, I. R., et al. (2013), Discovery of the action of a geophysical synchrotron in the Earth's Van Allen radiation belts, *Nat. Commun.*, *4*, 2795, doi:10.1038/ncomms3795.

Mann, I. R., et al. (2016), Explaining the dynamics of the ultra-relativistic third Van Allen radiation belt, *Nat. Phys.*, doi:10.1038/NPHYS3799.

Mauk, B. H., N. J. Fox, S. G. Kanekal, R. L. Kessel, D. G. Sibeck, and A. Ukhorskiy (2013), Science objectives and rationale for the radiation belt storm probes mission, *Space Sci. Rev.*, *179*, 3–27, doi:10.1007/s11214-012-9908-y.

Millan, R. M., R. P. Lin, D. M. Smith, and M. P. McCarthy (2007), Observation of relativistic electron precipitation during a rapid decrease of trapped relativistic electron flux, *Geophys. Res. Lett.*, *34*, L10101, doi:10.1029/2006GL028653.

Ni, B., et al. (2015), Variability of the pitch angle distribution of radiation belt ultrarelativistic electrons during and following intense geomagnetic storms: Van Allen Probes observations, *J. Geophys. Res. Space Physics*, *120*, 4863–4876, doi:10.1002/2015JA021065.

O'Brien, T., and M. Moldwin (2003), Empirical plasmapause models from magnetic indices, *Geophys. Res. Lett.*, *30*(4), 1152, doi:10.1029/2002GL016007.

Omura, Y., N. Furuya, and D. Summers (2007), Relativistic turning acceleration of resonant electrons by coherent whistler mode waves in a dipole magnetic field, *J. Geophys. Res.*, *112*, A06236, doi:10.1029/2006JA012243.

Omura, Y., Y. Miyashita, M. Yoshikawa, D. Summers, M. Hikishima, Y. Ebihara, and Y. Kubota (2015), Formation process of relativistic electron flux through interaction with chorus emissions in the Earth's innermagnetosphere, *J. Geophys. Res. Space Physics*, *120*, 9545–9562, doi:10.1002/2015JA021563.

Ozeke, L. G., I. R. Mann, K. R. Murphy, I. Jonathan Rae, and D. K. Milling (2014), Analytic expressions for ULF wave radiation belt radial diffusion coefficients, *J. Geophys. Res. Space Physics*, *119*, 1587–1605, doi:10.1002/2013JA019204.

Reeves, G. D., K. L. McAdams, R. H. W. Friedel, and T. P. O'Brien (2003), Acceleration and loss of relativistic electrons during geomagnetic storms, *Geophys. Res. Lett.*, *30*(10), 1529, doi:10.1029/2002GL016513.

Reeves, G. D., et al. (2013), Electron acceleration in the heart of the Van Allen radiation belts, *Science*, *341*(6149), 991–994, doi:10.1126/science.1237743.

Santolík, O., C. Kletzing, W. Kurth, G. Hospodarsky, and S. Bounds (2014), Fine structure of large-amplitude chorus wave packets, *Geophys. Res. Lett.*, *41*, 293–299, doi:10.1002/2013GL058889.

Selesnick, R. S., and J. B. Blake (2002), Relativistic electron drift shell splitting, *J. Geophys. Res.*, *107*(A9), 1265, doi:10.1029/2001JA009179.

Shprits, Y. Y., R. M. Thorne, R. Friedel, G. D. Reeves, J. Fennell, D. N. Baker, and S. G. Kanekal (2006), Outward radial diffusion driven by losses at magnetopause, *J. Geophys. Res.*, *111*, A11214, doi:10.1029/2006JA011657.

Shprits, Y. Y., D. Subbotin, and B. Ni (2009), Evolution of electron fluxes in the outer radiation belt computed with the VERB code, *J. Geophys. Res.*, *114*, A11209, doi:10.1029/2008JA013784.

Shue, J., et al. (1998), Magnetopause location under extreme solar wind conditions, *J. Geophys. Res.*, *103*, 17,691–17,700, doi:10.1029/98JA01103.

Sibeck, D. G., R. W. Mcentire, A. T. Y. Lui, R. E. Lopez, and S. M. Krimigis (1987), Magnetic field drift shell splitting' cause of unusual dayside particle pitch angle distributions during storms and substorms, *J. Geophys. Res.*, *92*, 13,485–13,497, doi:10.1029/JA092iA12p13485.

Spence, H. E., et al. (2013), Science goals and overview of the energetic particle, composition, and thermal plasma (ECT) suite on NASA's Radiation Belt Storm Probes (RBSP) mission, *Space Sci. Rev.*, *179*, 311–336, doi:10.1007/s11214-013-0007-5.

Su, Z., H. Zheng, and S. Wang (2009), Evolution of electron pitch angle distribution due to interactions with whistler mode chorus following substorm injections, *J. Geophys. Res.*, *114*, A08202, doi:10.1029/2009JA014269.

Su, Z., F. Xiao, H. Zheng, and S. Wang (2010a), Combined radial diffusion and adiabatic transport of radiation belt electrons with arbitrary pitch-angles, *J. Geophys. Res.*, *115*, A10249, doi:10.1029/2010JA015903.

Su, Z., F. Xiao, H. Zheng, and S. Wang (2010b), STEERB: A three-dimensional code for storm-time evolution of electron radiation belt, *J. Geophys. Res.*, *115*, A09208, doi:10.1029/2009JA015210.

Su, Z., F. Xiao, H. Zheng, and S. Wang (2011a), CRRES observation and STEERB simulation of the 9 October 1990 electron radiation belt dropout event, *Geophys. Res. Lett.*, *38*, L06106, doi:10.1029/2011GL046873.

Su, Z., F. Xiao, H. Zheng, and S. Wang (2011b), Radiation belt electron dynamics driven by adiabatic transport, radial diffusion, and wave-particle interactions, *J. Geophys. Res.*, *116*, A04205, doi:10.1029/2010JA016228.

Su, Z., H. Zheng, L. Chen, and S. Wang (2011c), Numerical simulations of storm-time outer radiation belt dynamics by wave-particle interactions including cross diffusion, *J. Atmos. Sol. Terr. Phys.*, *73*, 95–105, doi:10.1016/j.jastp.2009.08.002.

Su, Z., H. Zhu, F. Xiao, H. Zheng, C. Shen, Y. Wang, and S. Wang (2012), Bounce-averaged advection and diffusion coefficients for monochromatic electromagnetic ion cyclotron wave: Comparison between test-particle and quasi-linear models, *J. Geophys. Res.*, *117*, A09222, doi:10.1029/2012JA017917.

Su, Z., et al. (2014a), Quantifying the relative contributions of substorm injections and chorus waves to the rapid outward extension of electron radiation belt, *J. Geophys. Res. Space Physics*, *119*, 10,023–10,040, doi:10.1002/2014JA020709.

Su, Z., et al. (2014b), Nonstorm time dynamics of electron radiation belts observed by the Van Allen Probes, *Geophys. Res. Lett.*, *41*, 229–235, doi:10.1002/2013GL058912.

Su, Z., et al. (2014c), Intense duskside lower band chorus waves observed by Van Allen Probes: Generation and potential acceleration effect on radiation belt electrons, *J. Geophys. Res. Space Physics*, *119*, 4266–4273, doi:10.1002/2014JA019919.

Su, Z., et al. (2015), Ultra-low-frequency wave-driven diffusion of radiation belt relativistic electrons, *Nat. Commun.*, *6*, 10096, doi:10.1038/ncomms10096.

Su, Z., et al. (2016), Nonstorm time dropout of radiation belt electron fluxes on 24 September 2013, *J. Geophys. Res. Space Physics*, *121*, doi:10.1002/2016JA022546.

Summers, D., and Y. Omura (2007), Ultra-relativistic acceleration of electrons in planetary magnetospheres, *Geophys. Res. Lett.*, *34*, L24205, doi:10.1029/2007GL032226.

Summers, D., R. M. Thorne, and F. Xiao (1998), Relativistic theory of wave-particle resonant diffusion with application to electron acceleration in the magnetosphere, *J. Geophys. Res.*, *103*, 20,487–20,500, doi:10.1029/98JA01740.

Summers, D., C. Ma, N. P. Meredith, R. B. Horne, R. M. Thorne, D. Heynderickx, and R. R. Anderson (2002), Model of the energization of outer-zone electrons by whistler-mode chorus during the October 9, 1990 geomagnetic storm, *Geophys. Res. Lett.*, *29*(24), 2174, doi:10.1029/2002GL016039.

Thorne, R. M., B. Ni, X. Tao, R. B. Horne, and N. P. Meredith (2010), Scattering by chorus waves as the dominant cause of diffuse auroral precipitation, *Nature*, *467*, 943–946, doi:10.1038/nature09467.

Thorne, R. M., et al. (2013), Rapid local acceleration of relativistic radiation-belt electrons by magnetospheric chorus, *Nature*, *504*, 411–414, doi:10.1038/nature12889.

Tsyganenko, N. A., and M. I. Sitnov (2005), Modeling the dynamics of the inner magnetosphere during strong geomagnetic storms, *J. Geophys. Res.*, *110*, A03208, doi:10.1029/2004JA010798.

Wang, B., Z. Su, Y. Zhang, S. Shi, and G. Wang (2016), Nonlinear Landau resonant scattering of near-equatorially mirroring radiation belt electrons by oblique EMIC waves, *Geophys. Res. Lett.*, *43*, 3628–3636, doi:10.1002/2016GL068467.

West, J. H. I., R. M. Buck, and J. R. Walton (1973), Electron pitch angle distributions throughout the magnetosphere as observed on Ogo 5, *J. Geophys. Res.*, *78*, 1064–1081, doi:10.1029/JA078i007p01064.

Xiao, F., Z. Su, H. Zheng, and S. Wang (2009), Modeling of outer radiation belt electrons by multidimensional diffusion process, *J. Geophys. Res.*, *114*, A03201, doi:10.1029/2008JA013580.

Xiao, F., C. Yang, Z. Su, Q. Zhou, Z. He, Y. He, D. Baker, H. Spence, H. Funsten, and J. Blake (2015), Wave-driven butterfly distribution of Van Allen belt relativistic electrons, *Nat. Commun.*, *6*, 8590, doi:10.1038/ncomms9590.

Yu, J., L. Li, J. B. Cao, G. D. Reeves, D. N. Baker, and H. Spence (2016), The influences of solar wind pressure and interplanetary magnetic field on global magnetic field and outer radiation belt electrons, *Geophys. Res. Lett.*, *43*, 7319–7327, doi:10.1002/2016GL069029.

Zhao, H., X. Li, J. B. Blake, J. F. Fennell, S. G. Claudepierre, D. N. Baker, A. N. Jaynes, D. M. Malaspina, and S. G. Kanekal (2014), Peculiar pitch angle distribution of relativistic electrons in the inner radiation belt and slot region, *Geophys. Res. Lett.*, *41*, 2250–2257, doi:10.1002/2014GL059725.

Zhu, H., et al. (2015), Plasmatrough exohiss waves observed by Van Allen Probes: Evidence for leakage from plasmasphere and resonant scattering of radiation belt electrons, *Geophys. Res. Lett.*, *42*, 1012–1019, doi:10.1002/2014GL062964.